Quantum-number flow in multiparticle production*

Nobuyuki Murai
Department of Physics, McGill University, Montreal, Canada H3C 3G1

Tateaki Sasaki†
Department of Physics, University of Tokyo, Tokyo 113, Japan
(Received 2 November 1973; revised manuscript received 2 October 1974)

Conservation of quantum numbers at each vertex (or local conservation of quantum numbers) associates the rapidity dependence of inclusive spectra with the approach to the scaling limit in the central region within the framework of the multiperipheral model (MPM). A model incorporating various internal quantum numbers is developed by introducing quantum-number-flow states. We restore the properties (1) strong ordering of particles in rapidity and (2) threshold effect (production of a heavy pair requires a high threshold) of the MPM. Clustering in final states leads to a stronger energy dependence of the inclusive spectra as compared to a model where secondaries are produced directly. In pp collisions, the right order of magnitude of the rates of increase with energy among the π, K, and $\bar{p}$ inclusive spectra in the central region is reproduced in the incident-momentum region from 24 to 1000 GeV/c.

I. INTRODUCTION

Accumulating experimental data have stimulated systematic approaches[1-7] to inclusive distributions for various kinds of produced particles. Consider the inclusive reaction $p + p \to c_i + X$, where $c_1 = p$, $c_2 = \pi^+$, $c_3 = \pi^-$, $c_4 = K^+$, $c_5 = K^-$, and $c_6 = \bar{p}$. The distribution for c_i in rapidity space is observed to be broader than that of c_{i+1}.[8] Furthermore, indeed, scaling[9] is well satisfied for $p + p \to \pi + X$ in the fragmentation region. However, large corrections are required to reproduce the rise of the π spectrum with energy in the central region, as well as the more important energy dependence of the K and $\bar{p}$ spectra yields.[8] Our main problem is how to combine these two observed features, (1) the rapidity dependence of the inclusive spectra and (2) the approach to the scaling limit in the central region.

In the original version of the multiperipheral model[10,11] (MPM) it is natural to ascribe these properties (1) and (2) (see Refs. 12 and 13) to the difference of various objects exchanged in the MP chain, *where quantum numbers are conserved at each vertex*. This characteristic will be referred to as local conservation of quantum numbers. On the other hand, the MPM as well as the thermodynamical model[14] is, in some sense, a parent of *independent*-cluster-emission models,[15] which have been much discussed in relation to the two-particle correlations[16] and the associated multiplicities. An early success[17] of the multiperipheral cluster models[18] was attained in fitting the multiplicity distribution with a Poisson distribution incorporating clusters emitted uniformly along the rapidity axis.[19] Sometimes these clusters are regarded as usual resonances[20]: The so-called ω and ρ models, etc., are adopted to explain neutral-charged particle correlations. However, independent resonance emission would be an overabstraction of weakly correlated production, because quantum numbers should be conserved in the strong interactions between resonances. Moreover, clustering leads to a considerable reduction of the original multiplicity for resonances as compared to the final multiplicity. This implies that the quantum numbers of initial particles affect inclusive spectra strongly even in the central region through local conservation of quantum numbers.[21] Possible clusters emitted independently should be completely different[22] from resonances and should correspond to a certain saturation of the strong interactions. Our standpoint is against independent emission of resonancelike clusters, but in favor of local conservation of quantum numbers.

Thus, the aims of this paper are twofold: firstly, to investigate how important a role the local conservation of quantum numbers plays in explaining the experimental features (1) and (2) in the MPM, and secondly to examine the conjecture[21] that resonancelike clustering leads to strong energy dependence of inclusive distributions in the central region.

The present paper is organized as follows. We simplify the MPM by introducing quantum-number-flow[23] (QNF) states as an abstraction of exchanged particles in Sec. II. In this simplification we retain strong ordering of particles according to rapidity.[11] A threshold effect (production of a heavy pair requires a high threshold) is taken into account. In Sec. III numerical results are compared with experimental data of pp collisions in the cen-

tral region [the absolute value of center-of-mass (c.m.) rapidity is less than (the maximum value) − 1]. As an example of resonancelike-cluster models, we take up a vector-meson-dominance model[10,15,21] (VMDM), where pseudoscalar mesons are emitted through the mediation of vector mesons, as well as a model where secondaries are directly produced (PSM, the pseudoscalar-meson scheme). We summarize the results and give discussions in Sec. IV.

Although our numerical investigations concern pp collisions throughout this text, our model is more comprehensive in scope. It should be emphasized that it provides us also with many-particle inclusive distributions with various initial particles. Once QNF states are introduced as an abstraction of the MPM, the distributions of QNF in additive internal quantum-number space (furthermore, in rapidity space) can be reconstructed as an observed quantity (see the Appendix). Moreover, the distributions can be calculated in an independent emission model.[24] The title of the present paper represents our hope of such a potential.

II. THE MODEL

A. Formulation

Let us consider a multiperipheral chain with n final particles, whose links correspond to exchanged particles and initial particles at the ends (Fig. 1), and the contribution of the graph to an inclusive process. We make the strong-ordering assumption throughout this text that the particles' ordering in rapidity is their ordering along the multiperipheral chain. Even if the ith outgoing particle (Fig. 1) is definite, other particles (except at the ends) are not detected. Therefore, there are various choices of exchanged particles on each link. It would be easy to write down a formal equation of the MPM with multicomponents of internal quantum numbers. However, it is mathematically formidable to solve the equation. Some simplification is necessary.

Concentrating our attention on quantum numbers, we consider internal quantum-number states on each link, which are referred to as quantum-number-flow (QNF) states. Suppose that a link is

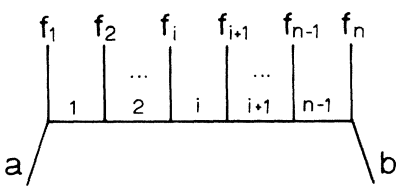

FIG. 1. Multiperipheral graph with n final particles.

in various QNF states with corresponding certain probabilities. The probability for a set of quantum numbers changes with the links from left to right (Fig. 1), and starts with 1 for the quantum numbers of the initial particle. Such simplification reminds us of probability processes, whose discrete time corresponds to the production steps, and of a sort of flow of quantum numbers. The concept of QNF will be reconstructed phenomenologically in the Appendix.

Let us now formulate the above outline. We employ Dirac's "bracket" notation, $\langle\alpha|$ or $|\alpha\rangle$, to denote an orthonormalized QNF state with α, which stands for a set of quantum numbers. We introduce an operator T, whose matrix element $\langle\beta|T|\alpha\rangle$ represents a (relative) transition probability from $|\alpha\rangle$ on one link to $|\beta\rangle$ on another link. We may either treat production amplitudes or probability functions (differential cross sections). We choose the latter for simplicity, although we are not strictly justified in this choice.[25] Then an inner product $\langle\alpha|\mu\rangle$ and the general state $|\mu\rangle$ is a probability, but not a probability amplitude.

In general, $\langle\beta|T|\alpha\rangle$ depends on i, n, rapidity y, and transverse momentum $p_\perp$ corresponding to the link for which $|\alpha\rangle$ and $|\beta\rangle$ are defined. Now we assume the following properties of T:

(i) The operator T relates a link to only the nearest neighbor ones. Further, the T connecting the ith link with the $(i-1)$th one is independent of i.

(ii) For simplicity, we neglect dependence on transverse momentum due to the small mean value.

(iii) The rapidity-dependent term is factorized out of T.

(iv) QNF states on any link are nonexotic. This condition restricts the dimension of T in its matrix representation.

(v) The operator T is real and symmetric. This property reflects the symmetry between a particle and its antiparticle in the fundamental dynamics.

It may be an oversimplification to make assumption (iii), which would be surely plausible for an isospin multiplet. In other words, we can see what effects arise from the local conservation of quantum numbers without energy dependence of propagators. Moreover, the formulas presented below are useful from a practical viewpoint, since the single operator T gives us various distributions, even many-particle correlation functions, with different incident particles.

We use assumption (i) in a multiplicative way. Then we have $\langle\alpha|T^{i-1}|\alpha\rangle$ on the ith link through "successive" production in the chain of $i-1$ particles (Fig. 1). Similarly, $\langle\bar{\beta}|T^{n-i}|\beta\rangle$ is the probability that $|\beta\rangle$ on the $(i+1)$th link transits to $|\bar{\beta}\rangle$, which is the antiparticle QNF state of another ini-

tial particle $|b\rangle$. Then we have the probability $P^{(n)}_{i,\gamma}$ of emission of quantum number γ at the ith final state:

$$P^{(n)}_{i,\gamma} = \sum_{\alpha,\beta} \frac{\langle \bar{b}|T^{n-i}|\beta\rangle\langle\beta|T_\gamma|\alpha\rangle\langle\alpha|T^{i-1}|a\rangle}{\langle \bar{b}|T^n|a\rangle}, \quad (2.1)$$

where

$$\langle\beta|T_\gamma|\alpha\rangle = \begin{cases} \langle\beta|T|\alpha\rangle, & \text{if vertex } \alpha \to \beta + \gamma \text{ is not zero} \\ 0, & \text{otherwise.} \end{cases} \quad (2.2)$$

Note that the multiplication of T corresponds to the summation over final particles. The natural assumption (v) enables us to make an exchange between a and b in (2.1) together with other corresponding quantities; i.e., the direction of QNF is reversible.

We introduce the abbreviated notation of operator fraction $A//B$:

$$\langle\alpha|A//B|\beta\rangle \equiv \langle\alpha|A|\beta\rangle / \langle\alpha|B|\beta\rangle. \quad (2.3)$$

In this notation, (2.1) is reduced to

$$P^{(n)}_{i,\gamma} = \langle \bar{b}|F_\gamma(i;n)|a\rangle, \quad (2.4)$$

with

$$F_\gamma(i;n) = T^{n-i}\,T_\gamma T^{i-1}//T^n. \quad (2.5)$$

Here we used completeness of the QNF states $\{|\alpha\rangle\}$.

It is of interest to give the double-particle distribution for $a+b \to f_{i,\gamma} + f_{j,\delta} + X$. Arguments similar to the ones above lead us to a formula for the quantum-number part of the double-particle spectrum with n final particles:

$$P^{(n)}_{i,\gamma;j,\delta} = \langle \bar{b}|T^{n-j}\,T_\delta T^{j-1-i}\,T_\gamma T^{i-1}//T^n|a\rangle. \quad (2.6)$$

This formula would be helpful in an investigation determining what role local conservation of quantum numbers plays in two-particle correlations.

In order to obtain a formula for the inclusive single-particle spectrum, we sum (2.1) over n and i, multiplying by the rapidity-dependent factor [see assumption (iii)]:

$$f_{ab\to\gamma}(y) = \sum_{n=2}^{\infty}\sum_{i=1}^{n} \int \prod_{l=1}^{n}{}' dy_l \langle \bar{b}|F_\gamma(i;n)|a\rangle \times \tau_n(Y_b, Y_a; y_n, \ldots, y_{i+1}, y, y_{i-1}, \ldots, y_1), \quad (2.7)$$

where the prime means the omission of dy_i $(=dy)$; $\tau_n(Y', Y; y_n, \ldots, y_{i+1}, y, y_{i-1}, \ldots, y_1)$ is the differential cross section for n particles to be produced at $y_1, y_2, \ldots, y_n$; and Y' and Y are the rapidities of the initial particles. The condition $y_n \geq \cdots \geq y_1$ is imposed due to the assumption of strong-ordering in rapidity. We propose two models for the rapidity-dependent factor τ_n in (A) and (B) of Sec. II B.

B. Two simple models for τ_n

(A) Omitting the integration over $\prod_{l=1}^{n'} dy_l$, we calculate (2.7) at n discrete points and interpolate the spectra. The points $\{y_i\}$ are equally spaced and are selected so as to satisfy the energy-momentum conservation constraints. The number n may be taken to be nearly the mean multiplicity. In carrying out (A), in practice, we impose the conditions

$$y_{i+1} - y_i = y_i - y_{i-1}, \quad (2.8)$$

$$\sum_{i=1}^{n} m \sinh y_i = 0, \quad \sum_{i=1}^{n} m \cosh y_i = \sqrt{s}, \quad (2.9)$$

with total c.m. energy $\sqrt{s}$; these conditions determine $\{y_i\}$ completely. It is assumed that all outgoing particles have the same longitudinal mass m; otherwise it is difficult to solve (2.9). Therefore, this prescription is appropriate only for the VMDM, where the differences of masses are small.

(B) We connect τ_n with the partial cross section σ_n as follows:

$$\int \prod_{i=1}^{n}{}' dy_i\, \tau_n(Y_b, Y_a; y_n, \ldots, y_{i+1}, y, y_{i-1}, \ldots, y_1) = \sigma_n \tilde{\Omega}_{n,i}(y), \quad (2.10)$$

where $\tilde{\Omega}_{n,i}(y)$ is the relativistic longitudinal phase-space volume. In the calculation of $\tilde{\Omega}_{n,i}(y)$ we fix the rapidity y of the ith particle in ordering of final particles according to rapidity and integrate over rapidities of other particles. Then $\tilde{\Omega}_{n,i}(y)$ is a function of y. The normalization is given by

$$\int \tilde{\Omega}_{n,i}(y)\,dy = 1. \quad (2.11)$$

We now assume the following expression for $\Omega_{n,i}(y)$:

$$\tilde{\Omega}_{n,i}(y) = \frac{n!\,(y_{\max} - y)^{n-i}(y - y_{\min})^i}{(y_{\max} - y_{\min})^n (n-i)!\,i!}, \quad (2.12)$$

where $y_{\max}$ and $y_{\min}$ are the upper and lower kinematical boundaries, respectively. Analytical expressions for $\tilde{\Omega}_{n,i}(y)$ derived from its definition are represented[26] in the improved Chew-Pignotti-De Tar[11,27] approximation. Unfortunately, these expressions yield good accuracy only for values of

n less than 10. The form (2.12) was compared with the more exact expressions in the region of their good accuracy and was found to give qualitative agreement.[26] Therefore, we shall employ (2.12) for convenience in practical calculations.

The partial cross section σ_n is parametrized as follows:

$$\sigma_n = \frac{\{G(s)\ln[(\sqrt{s}-m(2,n))(\sqrt{s}-m(1,n-1))/m_1 m_n]\}^{n-2}}{(n-2)![\sqrt{s}-m(2,n)][\sqrt{s}-m(1,n-1)]} \times A\,, \tag{2.13}$$

where s is the c.m. energy squared,

$$m(i,j)=\sum_{k=i}^{j} m_k\,,$$

and m_k is the longitudinal mass of the kth particle in order of rapidity. The above formula is suggested by the total phase-space volume at high energy. The parameter $G(s)$ corresponds to the coupling constant squared and is assumed to vary with s. The total mean multiplicity will be employed to determine $G(s)$ (Sec. III). Strictly speaking, $G(s)$ should not depend on energy in the MPM. However, we are interested in the role of local conservation of quantum numbers without possible bias coming from the defects of the MPM. Therefore, we adopt such a semiempirical σ_n. The over-all normalization factor A is given so as to have

$$\sum_{n=3}\sigma_n=\sigma_{\text{inel}}=\text{const.}$$

In order to see the effect of local conservation of quantum numbers clearly, we do not take account of the rising total cross section[28] observed recently. It is immediately clear that inclusive spectra are proportional to σ_{inel} within our framework.

III. RESULTS

A. High-energy limit

First we show consequences which are immediately clear in the high-energy limit. We made the assumption (i) in Sec. II A that transitions occur only between nearest neighbor links. Correlations of quantum numbers between distant links are, however, not vanishing. Once T is fixed, they depend on the number of links between the particles considered. In the high-energy limit, QNF states in the central region are controlled by T^n $(n\gg 1)$. Here we set forth analytical results in the region in this limit.

(1) It is plausible to assign squared Clebsch-Gordan coefficient to elements of $\{\langle\beta|T|\alpha\rangle\}$ in the same isomultiplet. Then charge independence holds for particle-production ratios.

(2) A particle-production ratio between different isomultiplets approaches a constant irrespective of initial particles. In general, this constant is not equal to 1 and is related to the eigenvector for the maximum eigenvalue of T.

(3) The production ratio of a particle to its antiparticle is 1. This feature is clear from the symmetry of T (assumption v) in Sec. II A.

B. Applications to *pp* collisions

The single-particle spectra in pp collisions are well investigated experimentally. The formula (2.7) will be applied to this actual reaction.

1. Simple models

As mentioned in Sec. I, we shall deal with the two models, the PSM where pseudoscalar mesons are produced directly and the VMDM where outgoing pseudoscalar mesons are mediated by vector mesons. The VMDM embodies a model where resonances are emitted almost uniformly along the rapidity axis.

Our numerical calculations are in the preliminary stage and may be considered a model calculation. We now consider a simple 3-quantum number system with isospin, baryon number, and strangeness. The QNF states do not necessarily correspond to particles. It is, however, convenient to use for these states the conventional notation of particles. We take account of the following sets of QNF states:

(π^+,π^0,π^-): isotriplet, nonstrange "mesons";
(K^+,K^0) and $(\bar{K}^0,K^-)$: isodoublet, strange "mesons";
(p,n) and $(\bar{n},\bar{p})$: "nucleons" and "antinucleons";
Y, $\bar{Y}$: isosinglet "hyperon" and "antihyperon."

Note that, in the PSM, we regard the (π^+,π^0,π^-) of QNF states as the summed contribution of the exchanged particles π and ρ and also do not distinguish K^* from K. In the VMDM we assume that (p,n), $(\bar{n},\bar{p})Y,\bar{Y}$, $(\rho^\pm,\rho^0)$, (K^{*+},K^{*0}), and $(\bar{K}^{*0},K^{*-})$ are produced as particles, neglecting ϕ, ω, and other resonances. These models, the PSM and the VMDM, are the simplest models to reproduce inclusive spectra for all stable charged hadrons. Even these minimum models require 13 components of QNF states.

Let us recall that the operator T determines transition probabilities. It is reasonable to assign the Clebsch-Gordan coefficients squared of SU_2 to the elements of the matrix $\{\langle\beta|T|\alpha\rangle\}$ in the same isomultiplet. Since T reflects, in some sense, underlying dynamics, it is inappropriate to use a higher symmetry (for example, SU_3) because of its observed breakdown. Thus we have the following explicit form of the matrix representation for T, with some elements undetermined:

$$T = \begin{array}{c} \\ p \\ n \\ Y \\ K^+ \\ K^0 \\ \pi^+ \\ \pi^0 \\ \pi^- \\ \bar{K}^0 \\ K^- \\ \bar{Y} \\ \bar{n} \\ \bar{p} \end{array} \begin{array}{c} \begin{array}{cccccccccccc} p & n & Y & K^+ & K^0 & \pi^+ & \pi^0 & \pi^- & \bar{K}^0 & K^- & \bar{Y} & \bar{n} & \bar{p} \end{array} \\ \begin{bmatrix} h & 2h & q & s & 0 & 2v & v & 0 & 0 & 0 & 0 & 0 & 0 \\ 2h & h & q & 0 & s & 0 & v & 2v & 0 & 0 & 0 & 0 & 0 \\ q & q & 0 & 0 & 0 & 0 & 0 & 0 & t & t & 0 & 0 & 0 \\ s & 0 & 0 & u & 2u & 2d & d & 0 & 0 & 0 & t & 0 & 0 \\ 0 & s & 0 & 2u & u & 0 & d & 2d & 0 & 0 & t & 0 & 0 \\ 2v & 0 & 0 & 2d & 0 & c & c & 0 & 2d & 0 & 0 & 2v & 0 \\ v & v & 0 & d & d & c & 0 & c & d & d & 0 & v & v \\ 0 & 2v & 0 & 0 & 2d & 0 & c & c & 0 & 2d & 0 & 0 & 2v \\ 0 & 0 & t & 0 & 0 & 2d & d & 0 & u & 2u & 0 & s & 0 \\ 0 & 0 & t & 0 & 0 & 0 & d & 2d & 2u & u & 0 & 0 & s \\ 0 & 0 & 0 & t & t & 0 & 0 & 0 & 0 & 0 & 0 & q & q \\ 0 & 0 & 0 & 0 & 0 & 2v & v & 0 & s & 0 & q & h & 2h \\ 0 & 0 & 0 & 0 & 0 & 0 & v & 2v & 0 & s & q & 2h & h \end{bmatrix} \end{array}, \tag{3.1}$$

where eight parameters, c, d, h, q, s, t, u, and v are to be fitted, aside from the over-all normalization. Therefore, we have essentially seven parameters.

We adopt model (B) in Sec. II B for the differential cross section τ_n in (2.7). We now give briefly the numerical values of the parameter $G(s)$ in (2.13) and a detailed prescription for calculations of $\tilde{\Omega}_{n,m}(y)$.

Table I shows the coupling constant squared $G(s)$, which is determined so as to reproduce the experimental total mean multiplicity. In both cases, the PSM and the VMDM, the total multiplicity $\langle n \rangle$ is evaluated with isospin invariance from the observed charged multiplicity.

The assumption of strong-ordering in rapidity appears in calculations of $\tilde{\Omega}_{n,m}(y)$ (Sec. III B 2). It is known empirically that, in many cases, the so-called leading particles carry away a large fraction of the available energy. To take account of this effect we assume that the particles emitted at the rapidities y_1 and y_n have the same mass as a proton. Furthermore, on account of a threshold effect, it is assumed that K (or K^*) or $\bar{p}$ is produced in a neighboring pair and that other outgoing particles except the leading particles are pions.

It is clear that we can apply the formula (2.12) to the cases $m \neq 1$. In Figs. 2(a) and 2(b) we depict inclusive spectra of the mth particle ($m = 1, 2, 3$) in order of rapidity, which are derived only from energy-momentum conservation constraints with the leading-particle effect. They are calculated under almost the same, but a somewhat simplified, prescription as compared with that in Ref. 26. The figures tell us that $\tilde{\Omega}_{n,m}(y)$ ($m \geq 2$) is applicable to the laboratory rapidity $y_{\text{lab}} \gtrsim 1$. This restriction is not inconsistent with current approaches: The two-component picture for multiparticle production is being widely used to describe various aspects of multiparticle production data. In such a picture, high-multiplicity events are imagined to occur through multiperipheral processes and to be observed in the central region.[28]

2. *Numerical results*

Our numerical calculations of (2.7) proceed through two steps: First, the matrix T is determined in a fit of inclusive spectra at incident laboratory energy 300 GeV in the PSM and at 1000 GeV in the VMDM. Then, the over-all normalization of σ_{inel} is given. Next, we have the energy dependence of the spectra without any adjustable parameters.

Figure 3(a) shows inclusive distributions for

TABLE I. Coupling constant $G(s)$ shown versus center-of-mass energies. The accompanying mean multiplicity is also indicated.

$\sqrt{s}$ (GeV)	G in PSM	$\langle n \rangle_{\text{PSM}}$	G in VMDM	$\langle n \rangle_{\text{VMDM}}$
4.93	1.26	4.3	0.70	3.2
6.85	1.38	5.6	0.70	3.9
8.77	1.41	6.6	0.75	4.5
13.78	1.44	8.4	0.80	5.6
23.78	1.50	10.7	0.86	7.0
43.37			0.90	8.4

charged particles in the PSM. When we set $c=1$ in (3.1), the remaining parameters are set as follows:

$$d=0.15,\quad h=0.25,\quad q=0.096,$$
$$s=0.096,\quad t=0.074,\quad u=0.15,\quad v=0.13, \tag{3.2}$$

which have been obtained after some trial and error.

In Fig. 3(b) are displayed inclusive spectra in the framework of VMDM. We have the following parameters;

$$d=0.205,\quad h=0.34,\quad q=0.13,$$
$$s=0.13,\quad t=0.10,\quad u=0.20,\quad v=0.18. \tag{3.3}$$

The "experimental" values in Fig. 3(b) should be commented on. We determine the total contribution $2M^+$ of ρ^+ and ρ^0 to the π^+ spectrum and $2M^-$ of ρ^- and ρ^0 to the π^- one in the following way: The ρ distribution in x space is assumed to be $(1-|x_\rho|)^\beta$. Here we denote by x_f Feynman's scaling variable[9] for a particle f. We set the effective values $\beta=1.6$ and 2.2 for $2M^+$ and $2M^-$ to reproduce the observed π^+ and π^- spectra fairly well, as partially shown in preceding works.[21,23] In order to facilitate comparison with theoretical curves we plot M^+ and M^-. For simplicity, we neglect the contribution of K^* to $M^\pm$. Isospin invariance imposes the following relations between the K^* and K spectra:

$$K^+=\tfrac{1}{3}(2K^{0*}+K^{+*}),\quad K^-=\tfrac{1}{3}(2\bar{K}^{0*}+K^{-*}),$$
$$K^0=\tfrac{1}{3}(2K^{+*}+K^{0*}),\quad \bar{K}^0=\tfrac{1}{3}(2K^{-*}+\bar{K}^{0*}), \tag{3.4}$$

where the spectra are indicated by the corresponding italic letters. Modification due to the decay process $(K^*\to K)$ would not be necessary because of the large mass of K.

It is immediately seen that the VMDM yields a better fit than the PSM. However, if we examine Fig. 3(b) in detail, even in the VMDM the calculated p spectrum is much less than that observed at $y_{\text{lab}}=1-1.5$. We expect that the diffraction component should fill up the discrepancy. It is difficult to come to a definite conclusion before refinement of τ_n [Eq. (2.7)]. The prescription (A) in Sec. II B provides us with the better fit [the dashed line in Fig. 3(b)] with the same parameters (3.3).

We are now in a position to examine the approach to the scaling limit in the pionization region. The central values of the spectra are less dependent on the choice between (A) and (B) than the shape. The

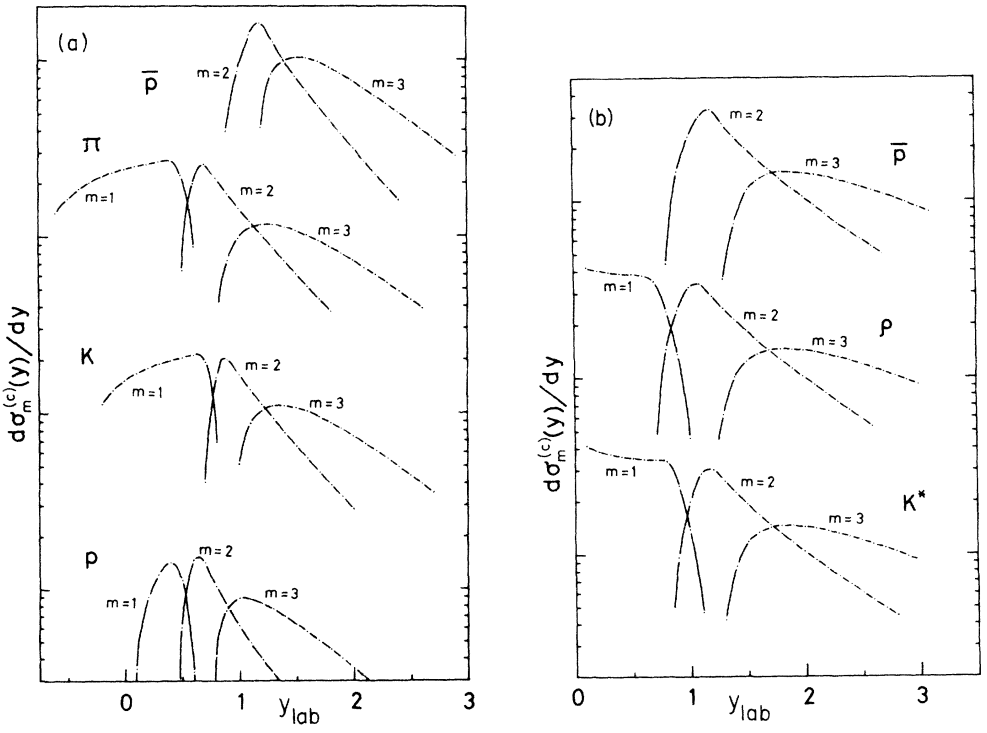

FIG. 2. (a) Inclusive distributions for the mth particle in ordering of rapidity at incident laboratory energy 300 GeV in the PSM, which are suggested only by phase-space volume. (b) Inclusive distributions for the mth particle in ordering of rapidity at 1000 GeV in the VMDM, which are derived from energy-momentum conservation constraints.

K^- and $\bar{p}$ distributions are compared with $M^0 = \frac{1}{2}(\rho^+ + \rho^-)$ and π^0 in Figs. 4(a) and 4(b), respectively. The VMDM gives the stronger dependence on energy. To see the central values ($y_{\text{c.m.}} = 0$) more clearly, we illustrate those for $M^0(\pi^0)$, K^-, and $\bar{p}$ versus energy in Fig. 5(a) and the particle-production ratios of K^- and $\bar{p}$ to all the emitted particles in Fig. 5(b). The difference between the PSM and VMDM is not so large as expected in a preceding work.[21] The stronger energy dependence can be attributed to two reasons: First, the parameter c is more dominant in the PSM than in the VMDM. Second, the mean multiplicity for resonances is reduced to about half of that for final particles.

It is seen from Table II that the VMDM can reproduce the observed increase of the π spectrum with energy, if the increase due to the resonance decay[21] is taken into account in addition to the rise from local conservation of quantum numbers. The calculated rise for K^- is about half of the empirical one and that for $\bar{p}$ about one-third. This implies that K^- and $\bar{p}$ production is suppressed at the lower energy more than required by local conservation of quantum numbers in the VMDM.

IV. CONCLUSIONS AND DISCUSSIONS

We have investigated effects of local conservation of quantum numbers along the rapidity axis by simplifying the MPM. In this simplification, we keep the following properties of the MPM:

(a) conservation of quantum numbers at each vertex,

(b) strong-ordering of particles in rapidity, and

(c) energy-momentum conservation and threshold effects.

We take up a vector-meson-dominance model (VMDM), as an example of cluster-emission models, as well as a model with final particles directly produced (PSM).

In conclusion, the right order of the rises among π, K, and $\bar{p}$ has been reproduced, although the increases with energy in the central region are quantitatively insufficient. The VMDM yields a stronger energy dependence than the PSM. If we demand that local conservation of quantum numbers should give the full increases observed, our simplest model should be improved in the following manner: (1) the average mass of clusters is larger

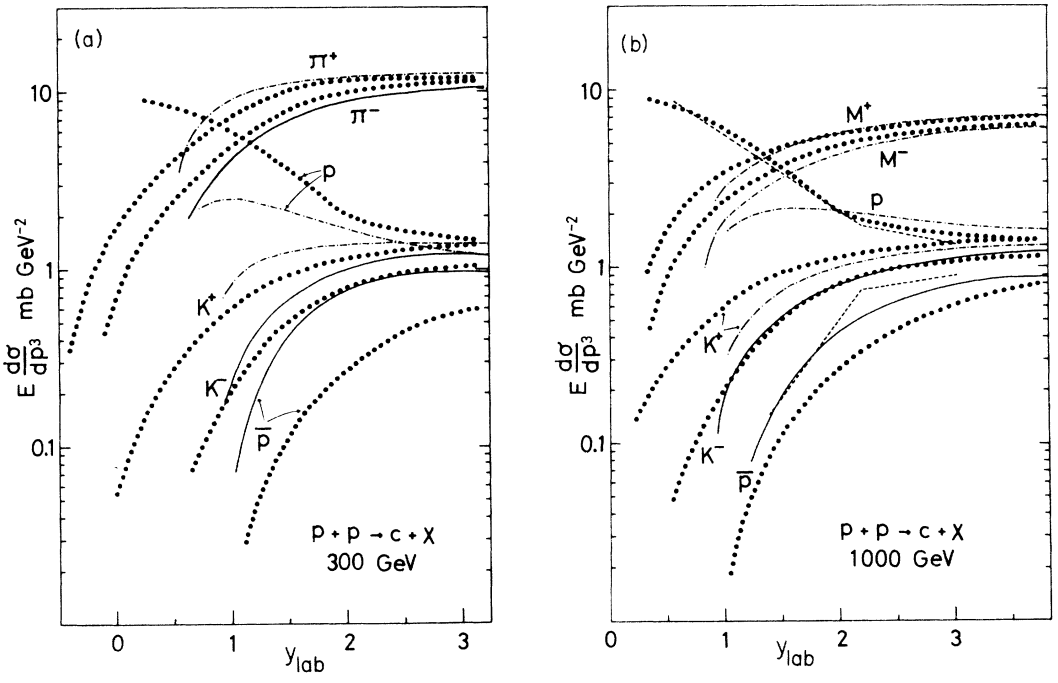

FIG. 3. (a) Inclusive spectra for the charged particles at 300 GeV in the PSM. The contribution of the first particle in order of rapidity is not included. The black circles represent experimental curves drawn schematically at $p_\perp = 0.4$ GeV/c (see Ref. 8) which are near the average transverse momentum. (b) Inclusive spectra for the charged particles at 1000 GeV in the VMDM. The contribution of the first particle in order of rapidity is not taken into account. "Experimental" black dots are drawn in the approximate center of the data at $\sqrt{s} = 23 \sim 53$ GeV (see Ref. 8). The typical deviations of the data from the dots are 10% for M, 30% for K^*, and 40% for $\bar{p}$. The dashed lines show spectra calculated by method (A) in Sec. II B.

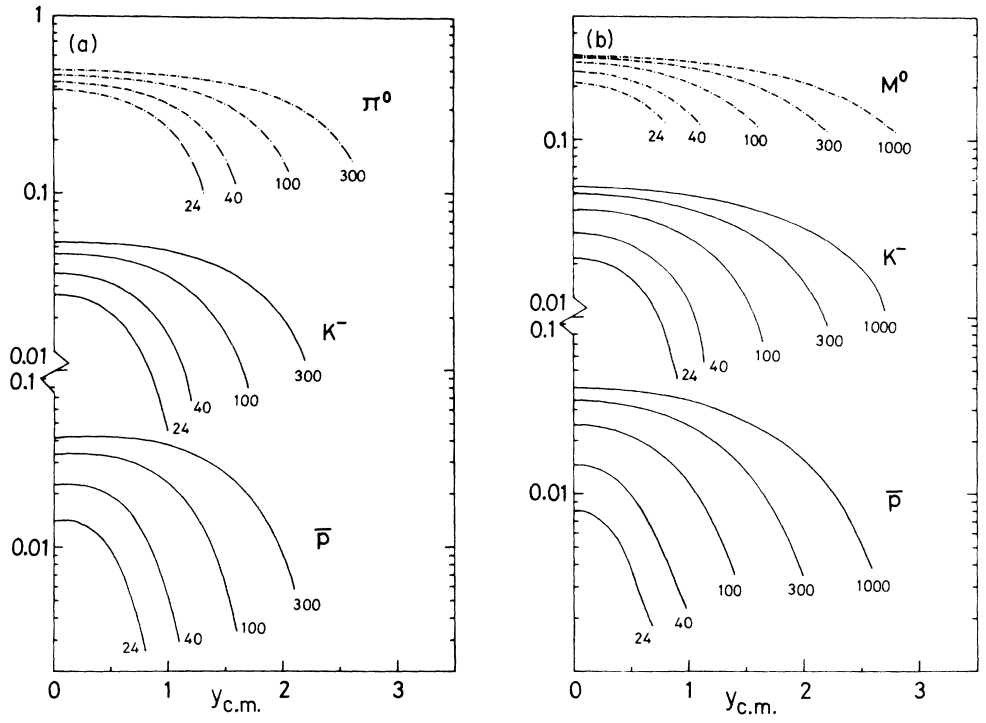

FIG. 4. (a) Inclusive distributions for π^0, K^-, and $\bar{p}$, which vary with energy in the PSM. (b) Inclusive distributions for M^0 $[M^0 = \frac{1}{2}(\rho^+ + \rho^0)]$, K^-, and $\bar{p}$, which vary with energy in the VMDM.

than those of the vector mesons. (2) The baryon resonances should be taken into account. In this article we have avoided the confusion of introducing more parameters in understanding the role of local conservation laws.

Our results imply that the quantum numbers of p affect the spectra in the central region even at CERN-ISR energies through conservation laws. They require a careful discrimination between "independent" emission models of clusters and multiperipheral cluster models with non-Pomeron objects exchanged.

In this framework it is not easy to find an exact analytical form[29] of the s dependence of the deviation Δf [Eq. (2.7)] from the scaling limit. Intuitively, Δf would be related to the mean multiplicity $\langle n \rangle$ in the manner $\Delta f \sim g\lambda^{\langle n \rangle}$ in the central region, where $\lambda(<1)$ and g are constants with respect to s.

We now consider the problem in which the central plateau is approached from below or from above. The answer depends on differences of quantum numbers between initial particles and the emitted particle. It is clear that the calculated distribution approaches the central plateau from above for the same kind of particle as the initial particles (for example, $p + p \to p + X$), or from below, if $(a\bar{c})$ and $(b\bar{c})$ are exotic in the inclusive process $a + b \to c + X$. These facts are also suggested by experiments. If $(a\bar{c})$ or $(b\bar{c})$ is nonexotic, we must make numerical calculations to obtain a definite answer, especially in the case where the initial particles are different from one another. It is necessary to examine which set of quantum number of initial particles penetrates dominantly from the fragmentation region to the central region through multiplication of the matrix T. Our experience is that the threshold effects (c) have a strong influence on the shape of the spectra in rapidity space; however, only local conservation of quantum numbers determines whether the scaling limit is reached from below

TABLE II. Ratios of invariant distributions for π^0, K^-, and $\bar{p}$ at incident laboratory energy 24 GeV to those at 1000 GeV, which are given at $y_{c.m.} = 0$ and $p_\perp = 0.4$ GeV/c. The empirical values are taken from small figures of Ref. 8. Their errors are about 30% for K^- and 40% for $\bar{p}$. The values of the K^- spectrum at 24 GeV are estimated by extrapolation.

	π^0	K^-	$\bar{p}$
VMDM	1.43	2.54	4.94
Experiment	1.61 [a]	5.4	16

[a] Average for π^+ and π^- and integrated over $p_\perp$.

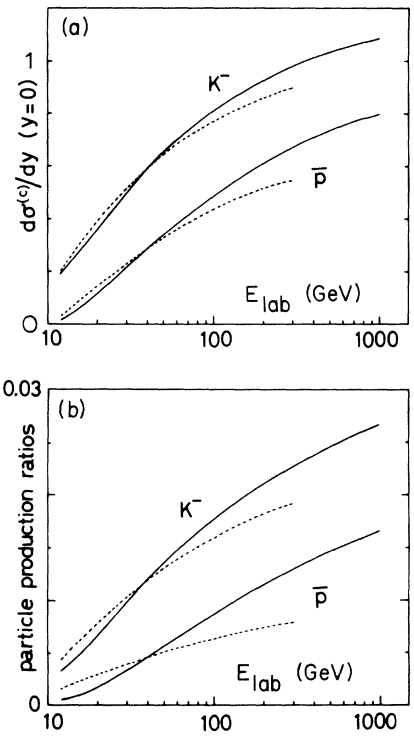

FIG. 5. (a) Inclusive spectra for K^- and $\bar{p}$ at the central point ($y_{c.m.}= 0$), which are indicated with solid curves for the VMDM and with dashed curves for the PSM. The values in the PSM are adjusted to those in the VMDM at 40 GeV to facilitate comparison. (b) Particle-production ratios of K^- and $\bar{p}$ to all produced particles, which are plotted versus energy with solid curves for the VDMD and with dashed curves for the PSM.

or from above.

If duality between resonances and exchanged particles holds in multiple production processes, we should consider infinitely many resonances and the VMDM should coincide with the PSM. However, current experimental data still cannot afford conclusive evidence of the duality in multiparticle production. At present, it is worthwhile to discuss the distinction between the PSM and the VMDM.

The usual Mueller-Regge analysis[30] gives the $s^{-1/4}$ behavior[29] for the deviation Δf in the central region if the Pomeron and meson trajectory are included. Blutner[31] has derived a $s^{-1/2}$ behavior,[29] using the version of the MPM of Caneschi and Pignotti, and Silverman and Tan.[32,13] In almost the same framework, Caneschi[1] has argued that the exponential cutoff in momentum transfer leads to an increase of the structure function f [Eq. (2.7)] due to the t_{min} effect. Various multiperipheral models differ with regard to the number of different exchanged objects. Many studies incorporate only isospin[4,7] or a few kinds of exchanged trajectories[12,13,31-33] inside the Regge chain with the dependence of propagators on subenergies (a few-channel model). By contrast, we have been concerned with an extreme model—a many-channel model without energy-dependent propagators.

Systematic approaches incorporating various quantum numbers have been made in the scheme of sequential decay of a fireball[2] and the thermodynamical model.[3] From the viewpoint of local conservation laws, the former scheme would be similar to the MPM considered in this text. However, there is an essential difference between them from the viewpoint of the structure of probability. In the MPM, as seen in (2.1), the probability that a set of quantum numbers is emitted includes a product of the left probability $\langle\alpha|T^{i-1}|a\rangle$ and the right probability $\langle\bar{b}|T^{n-i}|\beta\rangle$; that is, it depends on the quantum numbers of the two initial particles, especially at relatively low energies. On the other hand, in the fireball decay, the quantum numbers of a produced particle are affected by its parent fireball first produced through a single decay chain.

ACKNOWLEDGMENTS

One of the authors (N.M.) is thankful to Professor B. Margolis and Professor C. S. Lam, and to Dr. K. Kinoshita (Kyushu University), for enlightening discussions. One of the authors (T.S.) is grateful to Professor S. Nakamura for encouragement and to T. Shimada for useful discussions. The authors express their gratitude to Dr. J. Steinhoff and Dr. P. E. Heckman for careful readings of the manuscript and for critical comments, and to Dr. I. Moen for correcting the English.

APPENDIX

It may be interesting to reconstruct the concept of QNF as an experimental quantity. We start with the definition of charge flow to make the concept of QNF clear. Let us consider the following exclusive reaction:

$$a+b\to f_1+f_2+\cdots+f_n,\quad y_i\leq y_{i+1} \tag{A1}$$

where the final particle f_i is emitted with c.m. rapidity y_i. For simplicity, we neglect the dependence on transverse momentum due to the small mean value. We designate by ξ_i the charge of the particle f_i. Then, one can define exclusive QNF from f_i to f_{i+1} for an exclusive event as follows (see Fig. 1):

$$\mu_i^{(n)}=\xi_a-\sum_{j=1}^{i}\xi_j =-\left(\xi_b-\sum_{j=i+1}^{n}\xi_j\right). \tag{A2}$$

Possible values of $\mu_i^{(n)}$ are 0, ±1, ±2, ... A set of all exclusive reactions of the type (A1) determines the distributions $W_i^{(n)}$ of $\mu_i^{(n)}$ in charge space:

$$W_i^{(n)} = \begin{pmatrix} w_{i,-1}^{(n)} \\ w_{i,0}^{(n)} \\ w_{i,1}^{(n)} \end{pmatrix}, \tag{A3a}$$

$$\sum_{\mu} w_{i,\mu}^{(n)} = 1. \tag{A3b}$$

Here we denote by $w_{i,\mu}^{(n)}$ the probability, summed over possible $\{f_i\}$ with fixed $\{y_i\}$, that the value of the ith charge flow is μ $(=\mu_i^{(n)})$. The explicit dependence of $W_i^{(n)}$ on a, b and rapidity is suppressed in order to simplify the notation. Equation (A3b) gives the normalization.

There may be various possible definitions of the distribution $W_i^{(n)}(y)$ at a rapidity point y:

$$w_{i,\mu}^{(n)}(y) \propto \int_y^{y_{n\,\max}} dy_n \cdots \int_y^{y_{i+2}} dy_{i+1} \int_{y_{1\,\min}}^{y} dy_i \cdots \int_{y_{1\,\min}}^{y_2} dy_1 \,(\text{the number of events with } \mu_i^{(n)} = \mu), \tag{A4}$$

where $y_{n\,\max}$ is the maximum of y_n and $y_{1\,\min}$ the minimum of y_1. Further, we define the distribution independent of $\{y_i\}$:

$$\bar{W}_i^{(n)} \propto \int dy\, W_i^{(n)}(y). \tag{A5}$$

We impose the normalization condition on $W_i^{(n)}(y)$ and $\bar{W}_i^{(n)}$.

Additivity of charge permits us to determine uniquely the distribution $W_i^{(n)}$, $W_i^{(n)}(y)$, and $\bar{W}_i^{(n)}$ from experiments. This implies that powerful distinctions between various pictures of multiple production are made by comparing the empirical distributions with those peculiar to the pictures.[24] In contrast to the charge fluctuation at the central rapidity points,[34] the QNF concerns more detailed information on the transmission of charge. It is immediately clear that the above discussions can be easily generalized to other additive quantum numbers.

*Work supported in part by the National Research Council of Canada and the Department of Education of the Province of Quebec.

†Present address: Institute for Physical and Chemical Research, Wako City, Saitama 351, Japan.

[1]L. Caneschi, Nucl. Phys. B68, 77 (1974); E. J. Squires and D. M. Webber, Nuovo Cimento Lett. 7, 193 (1973).

[2]F. Csikor, I. Farkas, Z. Katona, and I. Montvay, Nucl. Phys. B74, 343 (1974); E.-M. Ilgenfritz and J. Kripfganz, *ibid.* B62, 141 (1973).

[3]J. Letessin and A. Tounsi, Nuovo Cimento 11A, 353 (1972); 13A, 557 (1973); 15A, 358 (1973).

[4]D. K. Campbell and S.-J. Chang, Phys. Rev. D 8, 2996 (1973).

[5]K. Kinoshita and H. Noda, Prog. Theor. Phys. 50, 915 (1973).

[6]R. F. Amann and M. L. Blackmon, Nucl. Phys. B55, 189 (1973); M. Koca, Nuovo Cimento Lett. 8, 735 (1973).

[7]E. Kyriakopoulos, Nuovo Cimento 20A, 537 (1973); 20A, 559 (1973).

[8]We restrict ourselves to enumerate the references whose data are used in the present paper. Since 1973 over twenty papers on pp experiments have been published: Bonn-Hamburg-München Collaboration, Nucl. Phys. B69, 454 (1974); ANL-FNAL-Ames-Michigan-Maryland Collaboration, Phys. Rev. Lett. 30, 574 (1973); CHLM Collaboration, Nucl. Phys. B51, 388 (1973); B56, 333 (1973); B72, 376 (1974); B73, 40 (1974); A. Bertin *et al.*, Phys. Lett. 41B, 201 (1972); M. G. Albrow *et al.*, *ibid.* 40B, 136 (1972); P. Capilluppi *et al.*, in *Colloque sur la physique hadronique aux energies des ISR, 1973,* edited by J. Soffer (C.N.R.S., Marseille, 1973); G. Giacomelli, in *Proceedings of the Canadian Institute of Particle Physics Summer School, 1973,* edited by R. Henzi and B. Margolis (McGill Univ., Montreal, 1973).

[9]R. P. Feynman, Phys. Rev. Lett. 23, 1415 (1969); J. Benecke, T. T. Chou, C. N. Yang, and E. Yen, Phys. Rev. 188, 2159 (1969).

[10]D. Amati, A. Stanghellini, and S. Fubini, Nuovo Cimento 26, 896 (1962); L. Bertocchi, S. Fubini, and M. Tonin, *ibid.* 25, 624 (1962); Chan Hong-Mo, J. Loskiewitz, and W. W. M. Allison, Nuovo Cimento 57A, 93 (1968).

[11]G. F. Chew and A. Pignotti, Phys. Rev. 176, 2112 (1968).

[12]R. F. Amann, Phys. Rev. Lett. 26, 1349 (1972).

[13]J. Arafune and H. Sugawara, Prog. Theor. Phys. 48, 1652 (1972).

[14]R. Hagedorn, CERN Report No. 71-12, 1971 (unpublished).

[15]C. Quigg and G. H. Thomas, Phys. Rev. D 7, 2752 (1973).

[16]J. Ranft and G. Ranft, Nucl. Phys. B53, 217 (1973); Phys. Lett. 45B, 43 (1973); 49B, 286 (1974); R. Slansky, Nucl. Phys. B73, 477 (1974); E. L. Berger, Phys. Lett. 49B, 369 (1974).

[17]C. P. Wang, Phys. Rev. 180, 1463 (1969); D. E. Lyon,

Jr., ANL Report No. ANL/HEP 7107 (unpublished); E. L. Berger, Phys. Rev. Lett. 29, 887 (1972).
[18]G. Ranft and J. Ranft, Phys. Lett. 32B, 207 (1970); A. Białas, K. Fiałkowski, and K. Zalewski, *ibid.* 45B, 337 (1973); J. Kripfganz, G. Ranft, and J. Ranft, Nucl. Phys. B56, 205 (1973); P. Pirilä and S. Pokorski, Nuovo Cimento Lett. 8, 141 (1973); C. J. Hammer, Phys. Rev. D 7, 2723 (1973); F. Hayot and A. Morel, Nucl. Phys. B68, 323 (1974); C. K. Chen, Phys. Rev. D 9, 1476 (1974).
[19]Now this success has become doubtful (see Table I).
[20]E. L. Berger, D. Horn, and G. H. Thomas, Phys. Rev. D 7, 1412 (1973); D. Horn and A. Schwimmer, Caltech report, 1972 (unpublished); O. Czyżewski and K. Rybicki, Nucl. Phys. B47, 633 (1972); D. Robertson and N. Sakai, Nuovo Cimento Lett. 7, 227 (1973); C. B. Chiu and K.-H. Wang, Phys. Rev. D 8, 2929 (1973); D. Drijard and S. Pokorski, Phys. Lett. 43B, 509 (1973).
[21]T. Sasaki and N. Murai, Phys. Rev. D 9, 3070 (1974); Prog. Theor. Phys. 50, 610 (1973).
[22]For example, S. Hasegawa, Prog. Theor. Phys. 26, 150 (1961).
[23]T. Sasaki and N. Murai, Nuovo Cimento Lett. 7, 129 (1973).
[24]N. Murai and T. Sasaki, Univ. of Tokyo Report No. UT-217 (unpublished). The present paper is a revision of part of this one.
[25]R. F. Amann and P. M. Shah, Phys. Lett. 42B, 353 (1972); J. Steinhoff, Nucl. Phys. B55, 132 (1973).
[26]N. Murai and T. Sasaki, McGill Univ. report (unpublished).
[27]C. E. De Tar, Phys. Rev. D 3, 128 (1971).
[28]U. Amaldi *et al.*, Phys. Lett. 44B, 112 (1973); Pisa-Stony Brook Collaboration, *ibid.* 44B, 119 (1973); Nuovo Cimento 17A, 735 (1973); Michigan-Berkeley (LBL) Collaboration, Phys. Rev. Lett. 32, 441 (1974).
[29]The $s^{-1/4}$ behavior is compiled by T. Ferbel, Phys. Rev. Lett. 29, 448 (1972), and the $s^{-1/2}$ behavior is compiled by H. Meyer and W. Struczinski, DESY Report No. DESY 72/40, 1972 (unpublished).
[30]A. H. Mueller, Phys. Rev. D 2, 2963 (1970).
[31]R. Blutner, Nucl. Phys. B73, 125 (1974). Many works are enumerated in this.
[32]L. Caneschi and A. Pignotti, Phys. Rev. 180, 1525 (1969); D. Silverman and Chung-I Tan, Nuovo Cimento 2A, 489 (1971); R. Michael Barnett and D. Silverman, Phys. Rev. D 8, 2108 (1973); D. Silverman, *ibid.* 2279 (1973).
[33]A. Pignotti and P. Ripa, Phys. Rev. Lett. 27, 1538 (1971). This model is a two-channel one with Pomeron.
[34]T. T. Chou and C. N. Yang, Phys. Rev. D 7, 1425 (1973).